Point defects in Sc_2O_3 thin films by ion beam sputtering

P. F. Langston,[1] E. Krous,[1] D. Schiltz,[1] D. Patel,[1] L. Emmert,[2] A. Markosyan,[3] B. Reagan,[1] K. Wernsing,[1] Y. Xu,[2] Z. Sun,[2] R. Route,[3] M. M. Fejer,[2] J. J. Rocca,[1] W. Rudolph,[2] and C. S. Menoni[1,*]

[1]Electrical and Computer Engineering, Colorado State University, Fort Collins, Colorado 80523, USA

[2]Department of Physics and Astronomy, University of New Mexico, Albuquerque, New Mexico 87131, USA

[3]E. L. Ginzton Laboratory, Stanford University, Stanford, California 94305, USA

*Corresponding author: Carmen.Menoni@colostate.edu

Received 4 September 2013; revised 9 December 2013; accepted 10 December 2013; posted 11 December 2013 (Doc. ID 196855); published 15 January 2014

We show that the concentration of oxygen interstitials trapped in Sc_2O_3 films by ion beam sputtering from metal targets can be controlled by modifying deposition conditions. We have identified point defects in the form of oxygen interstitials that are present in Sc_2O_3 films, in significantly high concentrations, i.e., $\sim 10^{18}$ cm^{-3}. These results show a correlation between the increase of oxygen interstitials and the increase in stress and optical absorption in the films. Sc_2O_3 films with the lowest stress and optical absorption loss at 1 μm wavelength were obtained when using a low oxygen partial pressure and low beam voltage.

OCIS codes: (310.0310) Thin films; (310.1860) Deposition and fabrication; (310.6860) Thin films, optical properties; (310.6870) Thin films, other properties.

http://dx.doi.org/10.1364/AO.53.00A276

1. Introduction

Sc_2O_3 is a transparent dielectric with a bandgap of ~6 eV, and a refractive index of ~2 at wavelengths around 1 μm [1]. For these characteristics, it is sought as the high index component of dielectric coatings operating at wavelengths ranging from the ultraviolet (UV) to the mid-infrared. Sc_2O_3 has been used in the fabrication of quarter-wave stacks and antireflection coatings in combination with SiO_2 and MgF_2 for UV applications [2]. Due to its high permittivity, Sc_2O_3 is also a candidate for replacement of SiO_2 as a gate oxide. Wang *et al.* [3] recently employed atomic layer deposition (ALD) to deposit Sc_2O_3 on AlGaN/GaN devices to achieve good electrical properties for transistor operation. However, ALD Sc_2O_3 was found to be sensitive to moisture and an Al_2O_3 blocking layer was required. Mixed oxides that incorporate Sc_2O_3 have now been reported. Yakovkina *et al.* [4] synthesized $(HfO_2)_{1-x}(Sc_2O_3)_x$ alloys as a replacement for the SiO_2 in metal–insulator–semiconductor devices. The authors found that chemical vapor deposition (CVD) of Hf–Sc–O films within a narrow range of Sc concentrations produced high permittivity and low current leakage, $\sim 10^{-8}$ A/cm^2, films. Sc_2O_3/SiO_2 mixed oxide films deposited by ion beam sputtering (IBS) have also been reported [5]. This work used oxide targets to produce amorphous films ranging from pure SiO_2 to Sc_2O_3. Investigations of the laser damage behavior showed that in the nanosecond pulse regime, the laser damage was governed by defect density and showed a large difference between Sc_2O_3 and SiO_2. In contrast, in the short pulse regime, laser damage behavior was found to be independent of composition [5].

In this work we describe a study of the optical and structural properties of amorphous Sc_2O_3 thin films deposited by IBS. In contrast to a recent report by

1559-128X/14/04A276-05$15.00/0

Mende *et al.* [5], we employ a Sc metal target to deposit the Sc_2O_3 oxide film [6,7]. Among the advantages of using metal targets is the ability to tailor process parameters such as oxygen partial pressure and ion beam energy. A main objective of this work has been to identify modifications in the Sc_2O_3 structural and optical properties that are linked with the deposition process parameters. The results show that point defects in the form of oxygen interstitials are present in Sc_2O_3 films in significantly high concentrations, i.e., $\sim 10^{18}$ cm^{-3}. The density of these defects varies with deposition conditions. The results show a correlation between the increase of oxygen interstitials and the increase in stress and absorption in the films. Sc_2O_3 films with the lowest stress and absorption loss at $\lambda = 1$ μm were obtained when using a low oxygen partial pressure and low beam voltage. Under these conditions, the density of the oxygen interstitials in the as-deposited Sc_2O_3 films is minimized.

2. Experimental

Thin films of Sc_2O_3 were grown by IBS using a Veeco Spector. In one set of runs the beam voltage of the main Ar sputtering source was set equal to 1250 V, the current was 600 mA, and the variable was the oxygen partial pressure. The O_2 partial pressure was varied from 2 to 40 μTorr. In a second set, the oxygen partial pressure was constant at 3 μTorr and the energy of the Ar sputtering ions was varied between 600 and 1250 eV. The target was Sc metal with 99.9% purity and Ta impurity of <0.05%. Sc_2O_3 single layers were grown on fused silica substrates with a surface roughness of 0.6 nm. The surface roughness was measured to be ~0.6 nm from scans obtained using a NovaScan ESPM 3D atomic force microscope (AFM) operated in tapping mode with a 5 μm × 5 μm scan area.

Glancing angle x-ray diffraction (GAXRD) and x-ray photoelectron spectroscopy (XPS) measurements were carried out to determine the degree of crystallinity and the composition of these films, respectively. The thicknesses and optical constants of the transparent films were determined using a combination of transmission and ellipsometric data. Deposited films had nearly constant thicknesses, (205 ± 7) nm, and were transparent. The refractive indices of all films at $\lambda = 1$ μm, extracted from ellipsometric measurements, were equal to 2. The magnitude and sign of the stress in the Sc_2O_3 films, grown on 1 mm thick fused silica substrates, were determined using a Twyman–Green interferometer. Fits of five phase-shifted interference patterns to Zernike polynomials were used to determine the radius of curvature of the film-substrate structure. Stress was calculated from the inverse of the radius of curvature [8]. The optical absorption of the films was measured at two different wavelengths, $\lambda = 1.064$ μm and $\lambda = 0.514$ μm, using the photothermal common-path interferometry (PCI) technique [9]. A pump beam at $\lambda = 1.064$ μm and $\lambda = 0.514$ μm was used to excite a thermal response in the coating, respectively, while common-path interference of a HeNe probe beam at $\lambda = 0.633$ μm allowed for detection of the absorption of the film at each pump wavelength.

Electron paramagnetic resonance (EPR) studies were carried out at room temperature using a Bruker EMX EPR spectrometer with 100 kHz field modulation. Films were deposited on thin fused silica slides and placed in a quartz sample tube. EPR spectra for each deposition condition were taken for nearly equivalent film volumes, in the same cavity, on the same day and with the microwave propagation normal to the film surface. The microwave frequency used to probe the spin populations was 9.6 GHz for the measurements taken. Background spectra confirmed that the bare substrates and quartz sample tube signals were insignificant compared to the signals measured from the Sc_2O_3 films. This small background signal was subtracted from the scans of the Sc_2O_3 films. The relative spin concentrations were determined from the relative areas of the absorption signals. The EasySpin MATLAB library was used to fit the spectra to extract a g-tensor [10,11]. (All the analytical tools employed in this report have been detailed elsewhere [10]).

3. Results and Discussion

Figure 1 shows x-ray diffraction (XRD) spectra from the set of films deposited at different oxygen partial pressures in the range of 2–38 μTorr. The most prominent feature in the XRD spectra is the (222) diffraction peak of the cubic Sc_2O_3. The films are considered amorphous, as the crystallite size was determined to be ~10 nm based on the full width at half-maximum (FWHM) of the (222) peak compared with the crystalline quartz standard. An increase of the oxygen partial pressure affects the spectra in two ways: the position of the (222) peak shifts toward smaller θ, and the FWHM of the (222) peak increases by approximately 50%. Increases in the FWHM could be due to reduction in the crystallite size, increased stress, or a combination of both. The shift of the diffraction peak toward smaller diffraction angles with increasing oxygen partial pressure indicates a change in the lattice constant that is correlated with increased compressive stress in the films. Analysis of the XRD spectra in the Sc_2O_3 samples deposited using different beam voltages showed the (222) peak shifted by ~0.1% and broadened by ~10% between 600 and 1000 V. Results from independent stress measurements are shown in Fig. 2. The stress varied from 0.55 to 0.75 GPa when the beam voltage was varied from 600 to 1250 V. The stress in the Sc_2O_3 films deposited using different oxygen partial pressures varied from 0.77 to 1.3 GPa. Thus, the combination of low oxygen partial pressure and low beam voltage results in Sc_2O_3 films with the lowest stress.

The Sc_2O_3 thin films were also characterized by XPS to assess the stoichiometry and bonding

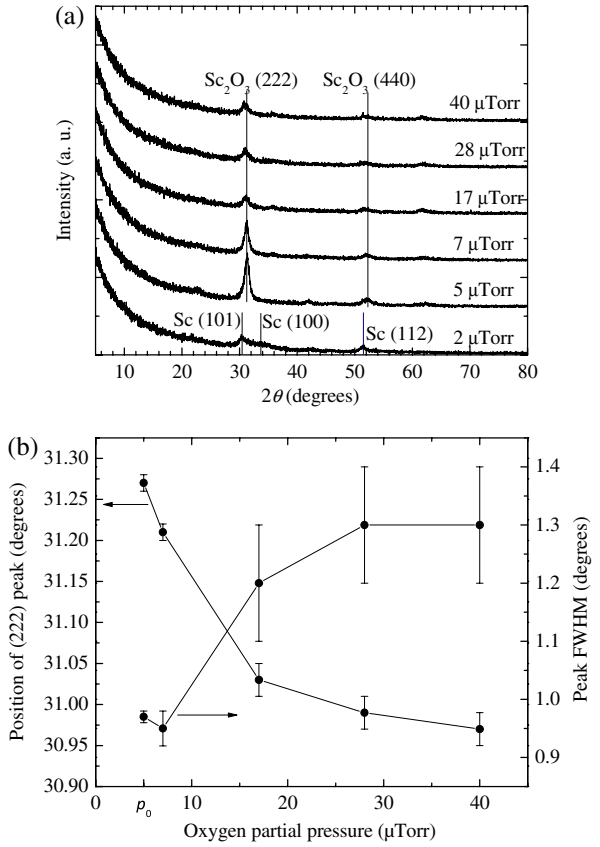

Fig. 1. (a) X-ray diffraction spectra of amorphous Sc_2O_3 for films deposited as a function of oxygen partial pressure. The film obtained at 2 μTorr shows diffraction features of crystalline scandium, and was opaque. All other films instead showed diffraction peaks that are identified with the (222) and (440) peaks of cubic Sc_2O_3. (b) The FWHM of the (222) peak increases and the peak position decreases to smaller angles with oxygen partial pressure, indicating an increase in the lattice parameter due to increased strain.

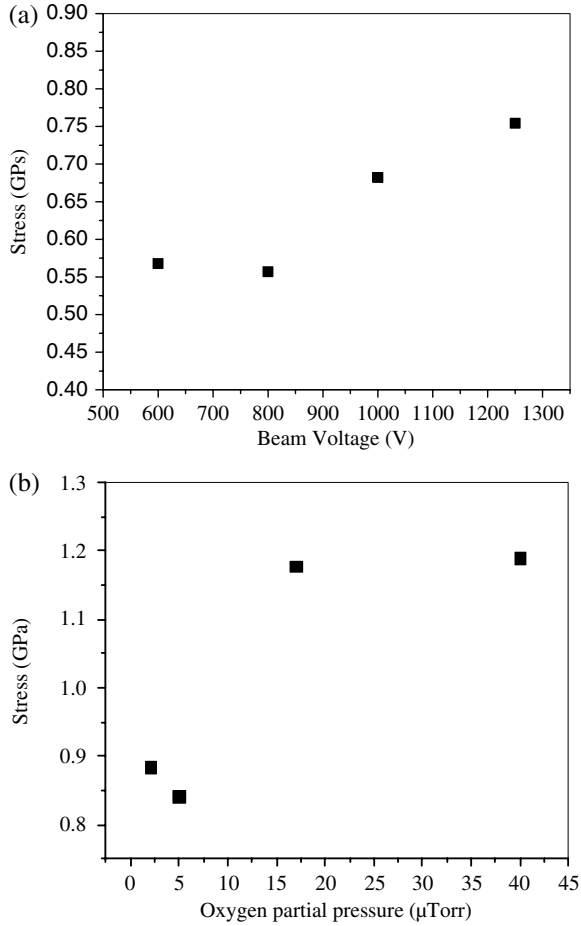

Fig. 2. Stress in Sc_2O_3 films with (a) variation in the beam voltage and (b) variation in the oxygen partial pressure.

environment. These results showed that the Sc in the IBS Sc_2O_3 films is in a single binding environment, while analysis of the O1s peak showed the oxygen had more than one signature for all the measured samples, indicating oxygen trapped in the films. The stoichiometry in the films varied from 1.72 to 1.84 for beam voltages of 600–1000 V, respectively. Instead, in the Sc_2O_3 films deposited using different oxygen partial pressures, the stoichiometry varied from 1.84 to 2.05, showing excess O_2 in the films [6].

Figure 3 illustrates the characteristics of the EPR spectra from samples deposited using different oxygen partial pressures. The signal was fitted using the EasySpin EPR MATLAB tool to extract the g-tensor component values, which for the dominant defect are $[g_{xx} = 2.017,\ g_{yy} = 2.017,\ g_{zz} = 2.055]$. This g-tensor corresponds to an oxygen interstitial defect [12]. EPR measurements on the samples deposited using beam voltages ranging from 600 to 1250 V produced the same results in terms of the defect characteristics. The density of oxygen interstitials obtained from the spectra in Fig. 3 for the two sets of samples is presented in Table 1. These oxygen interstitial defect densities are 2–5 times lower in the samples deposited at different beam voltages than found in the sample set deposited at different oxygen partial pressures.

Figure 4 plots the absorptivity or absorption coefficient (m^{-1}) at $\lambda = 1.064$ μm of the set of samples

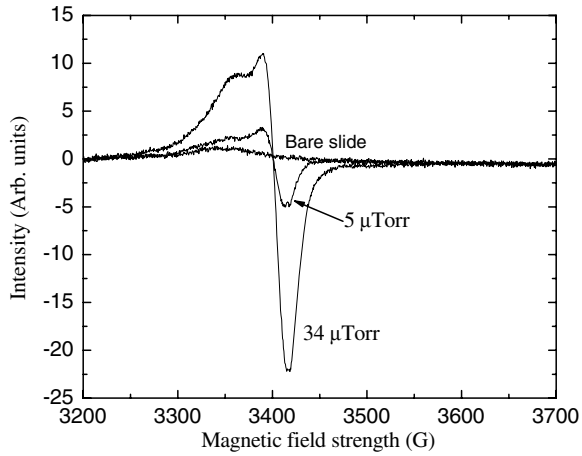

Fig. 3. EPR spectra for Sc_2O_3 films deposited at different oxygen partial pressures. A line shape analysis of the spectra is used to identify the defects and determine their density. An increase in the signal intensity correlates with a larger density of defects.

Table 1. Defect Density Determined from EPR for Sc_2O_3 Deposited with Different Beam Voltage and Sc_2O_3 Deposited with Different Oxygen Partial Pressure

Beam Voltage (V)	Defect Density (cm^{-3})
600	2.2×10^{18}
800	2.8×10^{18}
1000	3.8×10^{18}
1250	3.4×10^{18}
Oxygen Partial Pressure (μTorr)	**Defect Density (cm^{-3})**
5	1.3×10^{18}
7	3.9×10^{18}
38	1.04×10^{19}

deposited by varying the oxygen partial pressure and beam voltage, respectively. The absorption coefficient increased with oxygen partial pressure by about a factor of 4×, while it only increased by 2× with an increase in beam voltage. The variation of the absorption coefficient with process parameters correlates well with the variations in the density of oxygen interstitials. The data in Fig. 4 also show the absorptivity of the Sc_2O_3 films deposited using

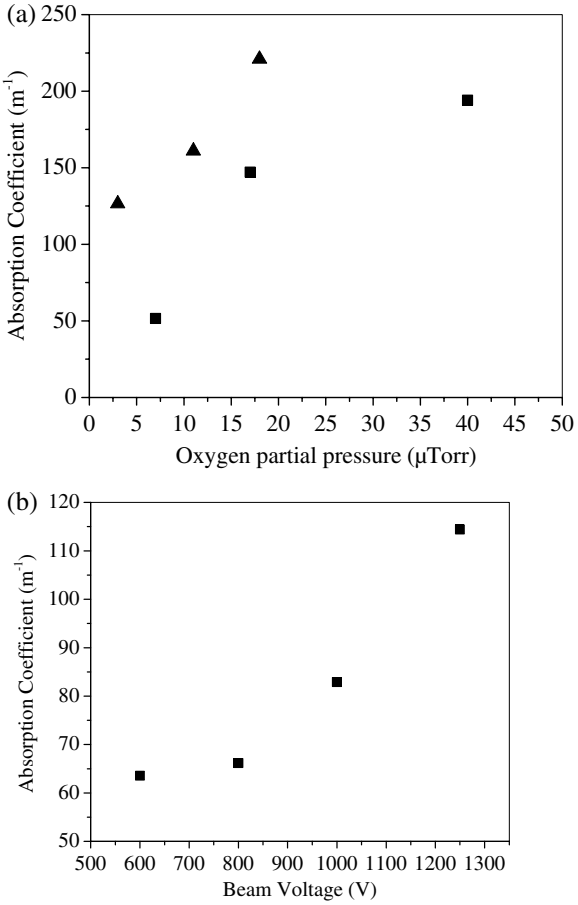

Fig. 4. Absorptivity of amorphous Sc_2O_3 films deposited using (a) different oxygen partial pressures and (b) different beam voltages. The triangle symbols identify a set of samples grown without use of the assist source. Both sets of data show an increase in absorptivity with oxygen partial pressure. The increase in absorptivity correlates with the increase in the density of oxygen defects.

different oxygen partial pressure with the use of the argon assist source during deposition. We attribute the decrease in absorptivity with the use of the assist source to preferential sputtering of oxygen and associated reduction in the density of oxygen point defects.

The absorptivity of the Sc_2O_3 films was also measured at $\lambda = 0.514$ μm. These results showed the absorptivity to be significantly larger, ~10×, than at $\lambda = 1.064$ μm (Fig. 5). Absorption in the large bandgap Sc_2O_3 films is due to the presence of trap states. These results suggest the presence of trap states at energies of 1.165 and at 2.412 eV near the band edges. We do not have sufficient information to discern whether these trap states are discrete energy states in k-space or a broad band as the absorption measurements were carried out at discrete wavelengths. Further studies are needed to identify the origin of the defect bands. This behavior is not unique to Sc_2O_3. We have shown that similar trap levels exist in IBS Ta_2O_5 and that the population and depopulation of these traps by electrons impacts the absorption of the films [13].

The parameter space in IBS is very broad as there are many degrees of freedom to realize thin films with similar optical and structural properties. In these studies we choose to vary the oxygen partial pressure because this is a critical parameter for reactive sputtering of metal oxides. We choose to vary the beam voltage because it has a direct impact on the energy distribution of the sputtered Sc target neutrals, and on the energy of reflected Ar neutrals [14]. The sputtering rate is also reduced when reducing the beam voltage. An increase of the oxygen partial pressure results in an increase of the oxide-to-metal target coverage and in the oxygen trapped within the growing film [10,15,16]. In both cases we have identified oxygen interstitials as being present. The concentration of oxygen interstitials was found

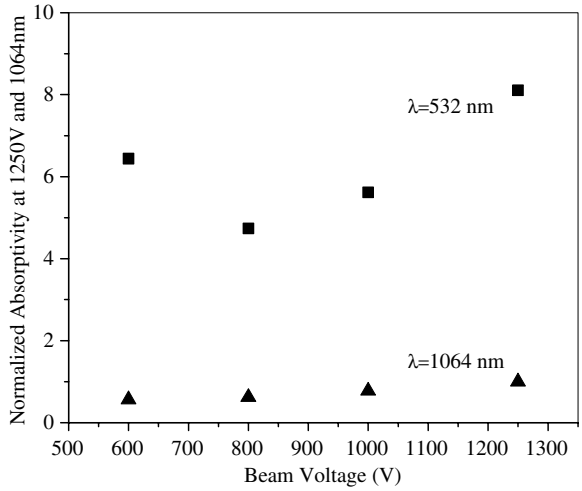

Fig. 5. Normalized absorptivity for Sc_2O_3 films at $\lambda = 1064$ nm and $\lambda = 514$ nm. The data were normalized to the value of the absorptivity at $\lambda = 1064$ nm for the film deposited at a beam voltage of 1250 V.

to be an order of magnitude lower in the set of Sc_2O_3 samples deposited using different beam voltages compared with the set of samples deposited using different oxygen partial pressure. The scaling of the absorption and stress in the films with increased oxygen partial pressure suggests that these defects play a role in affecting the optical and mechanical properties of the Sc_2O_3 thin films.

4. Conclusions

Isolating the role of defects in IBS metal oxide thin films in the optical and mechanical properties of amorphous metal oxides is quite challenging. In this work, we have identified oxygen interstitials. Signatures of these defects were also found in IBS HfO_2 and Ta_2O_5 and were observed to scale with the thickness of the film [13,17]. However, it is possible that other types of defects, such as oxygen vacancies, could be affecting absorption, and stress in the amorphous Sc_2O_3. In crystalline HfO_2, model predictions show there exists a distribution of deep and shallow defect states within the bandgap [18]. Different experiments are required to identify other types of bulk defects. Moreover, the effect of surface and interface defects in the absorption and stress in Sc_2O_3 amorphous thin films should not be discounted.

This work was supported by the Office of Naval Research and the High Energy Laser Program from the DoD Joint Technology Office, Grant Nos. N00014-09-1-0049, N0014-07-1-1068, and W911NF-11-1-0007. It made use of facilities developed through the NSF Engineering Research Center Program.

References

1. G. H. Liu, Y. X. Jin, H. B. He, and Z. X. Fan, "Effect of substrate temperatures on the optical properties of evaporated Sc_2O_3 thin films," Thin Solid Films **518**, 2920–2923 (2010).
2. F. Rainer, W. H. Lowdermilk, D. Milam, T. T. Hart, T. L. Lichtenstein, and C. K. Carniglia, "Scandium oxide coatings for high-power UV laser applications," Appl. Opt. **21**, 3685–3688 (1982).
3. X. W. Wang, O. I. Saadat, B. Xi, X. B. Lou, R. J. Molnar, T. Palacios, and R. G. Gordon, "Atomic layer deposition of Sc_2O_3 for passivating AlGaN/GaN high electron mobility transistor devices," Appl. Phys. Lett. **101**, 232109 (2012).
4. L. V. Yakovkina, T. P. Smirnova, V. O. Borisov, V. N. Kichai, and V. V. Kaichev, "Synthesis and properties of dielectric $(HfO_2)(1-x)$ (Sc_2O_3) (x) films," Inorg. Mater. **49**, 172–178 (2013).
5. M. Mende, S. Schrameyer, H. Ehlers, D. Ristau, and L. Gallais, "Laser damage resistance of ion-beam sputtered Sc_2O_3/SiO_2 mixture optical coatings," Appl. Opt. **52**, 1368–1376 (2013).
6. C. S. Menoni, E. M. Krous, D. Patel, P. Langston, J. Tollerud, D. N. Nguyen, L. A. Emmert, A. Markosyan, R. Route, M. Fejer, and W. Rudolph, "Advances in ion beam sputtered Sc_2O_3 for optical interference coatings," Proc. SPIE **7842**, 784202(2010).
7. C. S. Menoni, P. F. Langston, E. Krous, D. Patel, L. Emmert, A. Markosyan, B. Reagan, K. Wernsing, Y. Xu, Z. Sun, R. Route, M. M. Fejer, J. J. Rocca, and W. Rudolph, "What role do defects play in the laser damage behavior of metal oxides?" Proc. SPIE **8530**, 85300J (2012).
8. P. A. Flinn, D. S. Gardner, and W. D. Nix, "Measurement and interpretation of stress in aluminum-based metallization as a function of thermal history," IEEE Trans. Electron Devices **34**, 689–699 (1987).
9. A. Alexandrovski, M. Fejer, A. Markosian, and R. Route, "Photothermal common-path interferometry (PCI): new developments," Proc. SPIE **7193**, 71930D (2009).
10. E. M. Krous, "Characterization of Scandium Oxide thin films for use in interference coatings for high-power lasers operating in the near-infrared," M.S. thesis (Colorado State University, 2010).
11. S. Stoll and A. Schweiger, "EasySpin, a comprehensive software package for spectral simulation and analysis in EPR," J. Magn. Reson. **178**, 42–55 (2006).
12. R. C. Barklie and S. Wright, "Electron paramagnetic resonance characterization of defects in HfO_2 and ZrO_2 powders and films," J. Vac. Sci. Technol. B **27**, 317–320 (2009).
13. S. Markosyan, R. Route, M. M. Fejer, D. Patel, and C. Menoni, "Study of spontaneous and induced absorption in amorphous Ta_2O_5 and SiO_2 dielectric thin films," J. Appl. Phys. **113**, 133104 (2013).
14. E. Kay, F. Parmigiani, and W. Parrish, "Effect of energetic neutralized noble gas ions on the structure of ion beam sputtered thin metal films," J. Vac. Sci. Technol. A **5**, 44–51 (1987).
15. A. A. Barybin and V. I. Shapovalov, "Nonisothermal chemical model of reactive sputtering,"J. Appl. Phys. **101**, 054905 (2007).
16. S. Berg and T. Nyberg, "Fundamental understanding and modeling of reactive sputtering processes," Thin Solid Films **476**, 215–230 (2005).
17. B. Langdon, D. Patel, E. Krous, J. J. Rocca, C. S. Menoni, F. Tomasel, S. Kholi, P. R. McCurdy, P. Langston, and A. Ogloza, "Influence of process conditions on the optical properties HfO_2/SiO_2 thin films for high power laser coatings," Proc. SPIE **6720**, 67200X (2007).
18. A. S. Foster, F. L. Gejo, A. L. Shluger, and R. M. Nieminen, "Vacancy and interstitial defects in hafnia," Phys. Rev. B **65**, 174117 (2002).